Chapter 3

On protonation and methylation of benzene: A B3LYP DFT based study

In this chapter we have investigated mechanistic pathways for four different electrophilic addition processes with benzene (monoprotonation, diprotonation, monomethylation and dimethylation) in DFT framework. In all the cases, transition states have been isolated and characterized through intrinsic reaction coordinate calculations. Fukui functions, local softness values, local charge densities, different electrophile affinities, thermochemical parameters have been calculated and correlated. Fukui functions and local softness values have been found to be reliable descriptors for kinetically controlled products; whereas, prediction of thermodynamically controlled products can be made through local charge density values. Electrophile affinities are found to be additive and correlate well with thermochemical parameters.

3.1 Introduction

Most of the substitutions at aliphatic carbon are nucleophilic in nature, but the situation is reversed in case of an aromatic one. High π-electron density at the aromatic ring creates appropriate condition for electrophilic addition. Attachment of a positively charged species to benzene (Bz) ring occurs through a carbocation, which is a resonance hybrid known as sigma complex or arenium ion. This Wheland intermediate[1] has been isolated and characterized by many researchers. [2–5] Theoretical investigation on arenium ions is instrumental in the mechanistic study of reaction pathways involving such species. Olah and Khun[2] initiated such study, albeit from a classical point of view. Their work on isolation and characterization of different arenium ions serves as major land mark in the understanding of the mechanism of electrophilic attack on aromatic systems. Multistep character of electrophilic aromatic substitution has been ascertained by several such studies.[6] However, most of these studies were made in the gas phase to avoid the effect of complicating environment.

Protonation of benzene is the simplest example of electrophilic substitution to an aromatic ring. First experimental evidence of the existence of monoprotonated benzene (mpb) has been reported by Gold and Tye[4] and subsequently by Reid[5] through spectroscopic studies. Hehre and Pople carried out a thorough theoretical analysis on protonation of benzene and found the lowest energy structure for mpb where the proton is attached directly to one of the ring carbon atoms.[7] The possibility of diprotonated benzene (dpb) has first been predicted by Sumathy and Kryachko.[8] Diprotonated species can also be isolated due to their greater stability in comparison with the monoprotonated one. Through quantum chemical calculations, Sumathy and Kryachko extended their investigation to multi-protonation of benzene and have shown conclusively that mono, di even tri protonation of benzene can be possible, whereas tetra protonation leads to the opening of the aromatic ring. They concluded that meta diprotonated species with sigma complex type structure to be the global minima for BzH_2^{2+} potential energy surface. In a recent work, Roithova et al.[9] have studied the formation of doubly protonated species and

characterized it through mass spectrometry. They have also analyzed potential energy surface of different isomers of dpb through density functional formalism.

Beside proton, carbocation also acts as an electrophile to form arenium ion complexes. Because of the participation of carbocations in enzymatic reactions, much interest has been grown in the study of reaction dynamics of these reactions. Raos et al.[10] applied spin-coupled valence bond calculation on the reaction pathway for insertion of a methyl cation onto Bz, leading to the Wheland intermediate $BzCH_3^+$. This reaction has also been taken into account extensively by Miklis and coworkers where they predicted that CH_3^+ prefers a $\eta 1$ bonding with Bz rather than $\eta 6$ bonding.[11] Different forms of the arenium ions of this reaction were investigated through an ab initio direct molecular dynamics study by Ishikawa et al.[12] These results were compared with the results obtained through Car-Parrinello molecular dynamics by Zheng et al.[13]

Crux of our present work lies at the determination of the most plausible mechanistic pathways for different electrophilic additions to Bz in DFT framework. DFT-functionals which consider electron correlation appears effective in producing an accurate picture of electronic structures of reactants, products and transition states involved in the reaction mechanism. Reactivity at the sites of electrophilic attack has been quantified in terms of Fukui function, local softness, proton affinity etc., which are found supplementary to the mechanistic scheme of the reactions, intuited through electronic structure analysis. In this work we investigate mechanistic pathways for four different electrophilic addition reactions, (1) protonation of benzene, (2) protonation of monoprotonated benzene, (3) methylation of benzene and (4) methylation of monomethylated benzene (Scheme 3.1).

3.2 Methodology

A quantitative description of many electron systems can be obtained through rigorous post Hartree–Fock treatments; however, a reliable estimate of electronic properties can also be obtained in computationally economic density functional

framework. In this work, we explore mechanistic pathways for chosen electrophilic addition reactions through DFT studies. The geometries of all the reactants, products and transition states have been optimized using generalized gradient approach and split valence triple zeta diffused and polarized basis function. For all optimized structures, frequency analysis has been carried out at the same level of theory. This allows one to assign the reactants and products as genuine minima and shows at least one imaginary frequency for the transition states. To explicitly connect a particular transition state with relevant reactant(s) and product(s), the intrinsic reaction coordinate (IRC) has also been calculated for each transition state. The exchange correlation functional, which is used in this work, contains spurious electron self interaction, related to long range non-dynamic correlation of electron.[14] The self interaction error (SIE) influences the shape of the potential energy surface near the transition state by lowering the barrier height.[15] Being aware of this fact, our B3LYP results are further refined by carrying out single point calculations at MP2 level on the transition states.[16] Reactivity of any molecule can usually be described through global parameters such as electronegativity, hardness, softness etc. However, reactivity of a specific site can not directly be determined through these global reactivity parameters. Nevertheless, local reactivity parameters are found to be suitable to serve this purpose. In this study, we calculate local quantities such as Fukui function, local softness and charge density at different sites in a molecule. Regioselectivity for subsequent electrophilic attack at site k can be ascertained through evaluation of Fukui function (f_k^i),[17-19] an index which describes the reactivity towards an electrophilic attack and can be estimated using populations condensed to individual atoms (p_k) obtained through Mulliken population analysis as $f_k^- = [\rho_k(N) - \rho_k(N-1)]$, where N is the total number of electrons in the system.[20, 21] Local softness (s_k^i),[17-19] is another parameter for estimating the suitability of a specific site towards electrophilic attack, which is related to Fukui function as $s_k^i = f_k^i.S$ with $i = +$ or $-$, where S is the global softness.[22]

Proton affinity, which is the energy difference between protonated and deprotonated species is also suitable to explore mechanistic pathways.[8, 9, 23] This work includes the calculation of different electrophile affinities. These electrophile affinities

may in turn be related with the enthalpy of formation of different arenium ions. To draw this comparison, we also calculate the thermodynamic properties such as change in free energy and enthalpy.

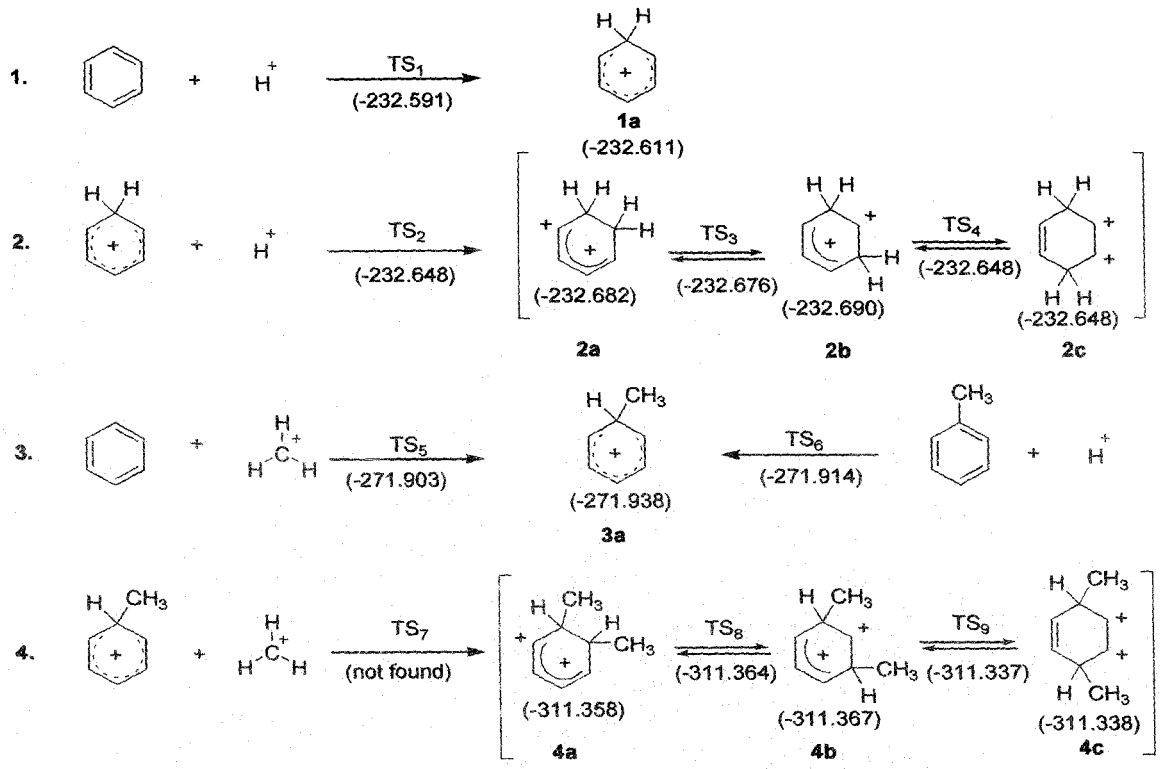

Scheme 3.1. Mechanistic pathways for the reactions under investigation. The engery values (a.u.) of the corresponding species are given in parenthesis.

3.3 Results and discussion

In this work, numerical calculations have been performed using UB3LYP exchange-correlational functional. Diffused basis functions have often been found to be effective in describing weak interaction among atoms.[24] Hence we use 6-311++G(d, p) basis function for a correct description of weak interactions which may prevail in the transition structures. The harmonic frequencies and zero point vibrational energies have been retained unscaled. These calculations are implemented through Gaussian 03W quantum chemical package.[25]

As evident from Scheme 3.1, six equivalent carbons in Bz are equally susceptible for electrophilic attack and protonation can take place arbitrarily at any one of them to produce mpb (1a), which has been found to have a methylene type of conformation where the proton resides on the C_{2v} symmetry axis; this observation is in good agreement with previous studies.[8] This is also well supported by the transition state TS_1. Methylenic protons in the transition state structure execute oscillation with a frequency of -1284 cm^{-1}, being equidistant from Bz ring. The proton affinity of the neutral benzene takes the value of 188 kcal/mol. The energy profile of this protonation process is given in Figure 3.1.

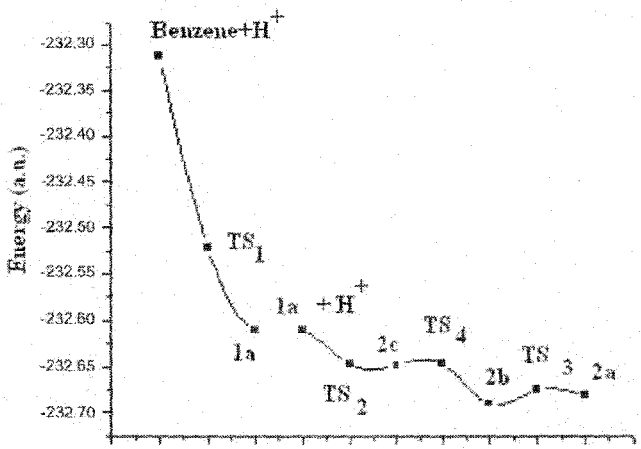

Figure 3.1 Energy ordering of reactants, products and transition states of protonation and diprotonation reactions

A monoprotonated species gives rise to the probability of three diprotonated isomers ortho (2a), meta (2b), and para (2c). From the energy values, displayed in Scheme 3.1, it is clear that among these three isomers, meta isomer is the most stable followed by ortho and para. The low energy barriers among the ortho, para and meta isomers facilitate proton walk among the sites and hence an equilibrium among the isomers of dpb is established. The energy ordering of the isomers can be viewed in Figure 3.1. Nucleophilicity of carbon centers in monoprotonated species is quantified in terms of Fukui functions (Table 3.1). Higher the value of Fukui function (f_k^-), greater is the probability of electrophilic attack at site k. In mpb, calculated Fukui functions predict highest nucleophilicity for the para position followed by meta and ortho. Apart from Fukui functions, we have also calculated local softness values for each carbon centers in

mpb (Table 3.1), which show the same trend. Further protonation of mpb proceeds through TS_2 which shows an imaginary frequency of -286 cm^{-1} originating from the oscillation of proton in between meta and para positions. Intrinsic reaction coordinate (IRC) study of the second reaction shows that the incoming proton prefers para position, and hence para disubstituted isomer seems to be kinetically controlled product. This is exactly suggested by Fukui functions and local softness values. This observation may initially appear contradictory to the energy values shown in Scheme 3.1. Nevertheless, meta isomer of dpb is the thermodynamically controlled product. Highest value of charge density at the meta position of mpb (Table 3.1) also supports this observation. Owing to the largest local reactivity parameters, para position becomes most susceptible to proton attack. Once H^+ attacks the para position, an interstitial proton transfer may follow, through a bridged intermediate. Ultimately thermodynamically stable meta di-substituted

Table 3.1

Fukui functions at different positions of protonated (1a) and methylated benzenium ion (3a)

Protonated benzene				Methylated benzene			
position	Softness	Fukui Function	Charge density	position	Softness	Fukui Function	Charge density
Ortho	0.937	0.151	0.586	Ortho	10.524	1.678	0.487
Meta	1.707	0.275	−0.515	Meta	6.592	1.051	−0.590
Para	1.993	0.321	0.300	Para	5.827	0.929	0.181

benzene is formed via transition state TS_4. Frequency calculation of TS_4 shows one negative frequency of -287 cm^{-1} which originates from the proton oscillation in between meta and para positions. One of the hydrogens in meta position of 2b can also migrate to ortho position through TS_3, which has one imaginary frequency of -540 cm^{-1}. Relative stabilities of different species involved in this diprotonation reaction are displayed in Figure 3.1. Proton affinity values of mpb as displayed in Table 3.2, also show highest and lowest degree of proton affinity in meta and para positions, respectively, supplementing the above fact. From the proton affinity values, second protonation to mpb appears less favorable than the first protonation. We also calculate the diproton affinity of Bz (Table

3.2). From Table 3.2, it is clear that the proton affinities follow the additivity rule. Free energy changes (ΔG) of reactions discussed above are tabulated in Table 3.3. The ΔG value in the formation of diprotonated benzene from monoprotonated species is maximum negative in case of meta di protonation, which stands for the spontaneity of that reaction. In dpb, negative ΔG values in the interconversion of isomers indicate a tendency of the reaction towards the meta isomer. Negative values of ΔH (Table 3.3) are found to have the same trend for conversions 1a→2a, 1a→2b and 1a→2c as that of their proton affinity values (Table 3.2). Positive values of proton affinities reflect higher stabilities of protonated species and hence exothermic nature of the reactions is well explicable.

Table 3.2

Proton affinity values of Bz, mpb (1a) and diproton affinity of bz. In the parentheses previously reported values and corresponding references are given.

Species		Proton affinity (kcal/mol)	Species		Diproton affinity (kcal/mole)
Benzene		188.269 (187.9)[7]	Benzene	Ortho	232.367
mpb	Ortho	44.098 (39.20)[9]		Meta	237.696
	Meta	49.427 (50.73)[9]		Para	211.506
	Para	23.237 (25.376)[9]			

Monomethylated benzene (mmb) (3a) can be obtained by reacting CH_3^+ to benzene through Friedel–Crafts type of reaction. An alternative route of getting 3a is obviously through addition of H^+ with toluene. Almost same energy of transition states TS_5 and TS_6 (Figure 3.2) predict equal probability of both routes. Nonetheless, in the second route, reaction coordinate is much steeper than that in the first one, and hence the rate through the second route should be higher. TS_5 has two imaginary frequencies, one of -261 cm^{-1} with relative intensity very small 0.01 and other -93 cm^{-1} with relative intensity 0.23. As a consequence, the higher intensity vibration would lead to the product. The methyl cation affinity (MCA) of benzene has been found to be 85 kcal/mol, which is in well agreement with the earlier results.[23]

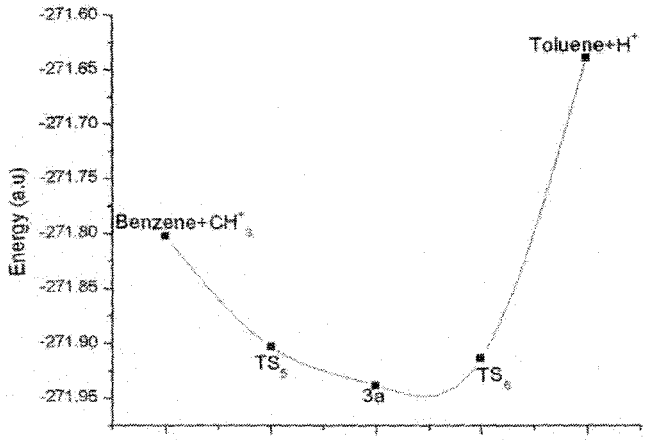

Figure 3.2 Energy ordering of reactants, products and transition states of monomethylation reaction.

This methylated benzene when subjected to further methylation, three isomers ortho (4a), meta (4b) and para (4c) may result. Energy values of optimized geometries of these three isomers reveal the meta to be the most stable (Scheme 3.1). However, softness and Fukui function calculations indicate a facilitating ortho attack (Table 3.1). To seek the transition state (TS_7) of this reaction, a methyl cation is suspended over monomethylated benzenium ion and output of the computation shows that the cation is attached to the ortho position; however, planarity of the benzene ring is lost (Figure 3.4). This puckeredness arises due to steric interaction between two methyl fragments in ortho position. To ensure this argument, we expose the monomethylated benzenium ion to a proton and the obtained transition state in this process shows that the proton is nearer to the ortho position as expected. The frequency of this transition state (-551 cm^{-1}) shows an oscillation of the proton between ortho and meta position keeping the planarity of the benzene ring intact. Leaving ortho position for obvious reason as described above, and through closer inspection of Table 3.1, one can surmise that the meta position will be the next preferred site for electrophilic attack and thus the meta isomer predominates (Scheme 3.1). The highest charge density value (Table 3.1) at meta position of methylated benzeneum ion also predicts the meta isomer to be the thermodynamically controlled product. Nevertheless, ortho and para isomers will be in equilibrium with meta dimethylated dication as can be seen from Figure 3.3. Inter conversion between ortho and

meta dimethylated benzene takes place through TS_8. It has one imaginary frequency of $-147\ cm^{-1}$. In this transition state, methyl group is placed in equitable distance from ortho and meta position and the negative frequency arises due to an unusual rotation of methyl group therein. Meta to para interconversion takes place through the transition state, TS_9 which is characterized by $-153\ cm^{-1}$ and the corresponding oscillation is executed between para and meta positions. The analysis of methyl cation affinity (MCA) strongly indicates it should exhibit the same additivity feature as that of the proton affinity, this is also apparent from Table 3.4 Thermochemical analysis of dimethylation reaction shows a positive change in free energy (Table 3.3). This observation suggests the requirement of activation energy for occurrence of the reactions as also shown by the energy profile of these reactions (Figure 3.3). However, free energy change for the interconversion between the different isomers of dimethylated species is negative, which indicates that ortho and para isomers can easily switch over to the energy-minimized meta isomer. Unlike diprotonation, dimethylation produces positive ΔH values (Table 3.3) and justifiably correspond to negative values of methyl cation affinities (Table 3.4).

Table 3.3
Free energy and enthalpy change of the reactions depicted in scheme 3.1

Conversion	ΔG (kcal/mol)	ΔH (kcal/mol)
Benzene→1a	−157.508	−155.939
1a→2a	−93.500	−92.434
1a→2b	−98.521	−97.712
1a→2c	−75.302	−73.865
2a→2b	−5.020	−5.279
2c→2b	−23.846	−23.847
Benzene + CH_3^+→3a	−99.776	−109.255
Toluene + H^+→3a	−180.098	−180.706
3a→4a	56.477	47.381
3a→4b	50.829	41.607
3a→4c	69.027	59.614
4a→4b	−5.648	−5.774
4c→4b	−17.571	−18.007

Table 3.4

Methyl cation affinity values of Bz, mmb (3a) and dimethyl cation affinity values of Bz. In the parenthesis previously reported value and corresponding reference is given.

Species		Methyl cation affinity (kcal/mol)	Species		Dimethyl cation affinity (kcal/mol)
Benzene		85.051 (81.4)[23]	Benzene	Ortho	40.267
mmb	Ortho	−44.784		Meta	45.871
	Meta	−39.180		Para	27.420
	Para	−57.631			

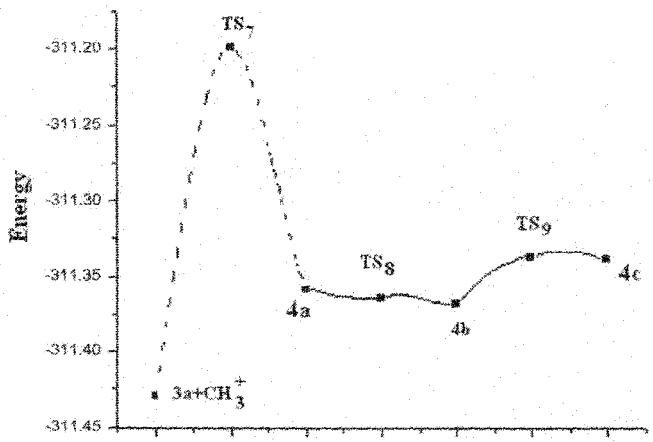

Figure 3.3 Energy ordering of reactants, products and transition states of dimethylation reaction.

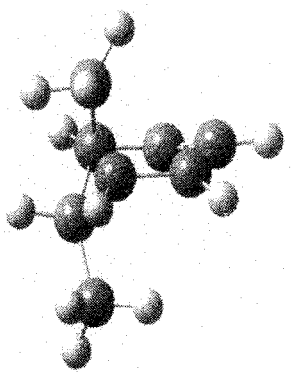

Figure 3.4 Puckered structure of TS_7.

As, the applied functional is reported to be inadequate in producing an accurate picture of potential energy surface,[14-16] the results have been compared with single point MP2 calculations on UB3LYP optimized geometries. Plotting of MP2 energies of the reactant, transition state and products reproduce the energy ordering of DFT functional, but with an overall scaled down representation. Comparison of DFT and post Hartree–Fock results are given in Tables 3.5 and 3.6.

Table 3.5

Energy of the transition states at UB3LYP and MP2 level. In the parentheses previously reported values and corresponding references are given.

Species	UB3LYP(a.u.)	MP2(a.u.)	Energy difference (a.u)
TS_1	−232.591	−231.860	0.731
TS_2	−232.648	−232.911	0.737
TS_3	−232.676 (−232.676)[9]	−232.930	0.746
TS_4	−232.648 (−232.652)[9]	−231.911	0.737
TS_5	−271.903	−271.043	0.86
TS_6	−271.914	−271.055	0.859
TS_8	−311.364	−310.364	1.000
TS_9	−311.337	−310.344	0.993

Table 3.6

Energy of different reactants and products at UB3LYP and MP2 level. In the parentheses previously reported values and corresponding references are given.

Species	UB3LYP (a.u)	MP2 (a.u.)	Energy difference (a.u.)
1a	−232.611	−231.871	0.740
2a	−232.682 (−232.681)[9]	−231.929	0.753
2b	−232.690 (−232.689)[9]	−231.938	0.752
2c	−232.648 (−232.651)[9]	−231.909	0.739
3a	−271.938 (−291.925)[11]	−271.072	0.866
4a	−311.358	−310.361	0.997
4b	−311.367	−310.363	1.004
4c	−311.338	−310.347	0.991

3.4 Summary

In this work we have studied electrophilic addition to benzene within DFT framework using UB3LYP hybrid functional and 6-311++G(d, p) basis function. The results reflect the same trend of mechanistic pathways in cases of diprotonation and dimethylation of benzene. In both the reactions the most stable product is a meta disubstituted one, followed by ortho and para. This is also well supported by simple valence bond based qualitative approach. In this approach, one can readily find only one possible structure for para disubstituted product in which two positive charges are geminal. In ortho and meta disubstituted products two resonating structures could be found; however, in case of ortho in one of these structures again charges are on neighboring sites, whereas, in case of meta isomer in none of them charges are adjacent. This clearly points out the meta disubstituted product to be most favorable energetically followed by ortho and para. This is also supported by local charge density values. Nevertheless, in case of diprotonation reaction the para isomer has been found to be kinetically controlled product, whereas the ortho one is the same for dimethylation reaction, which is also supported by the highest value of Fukui functions and local softness values in ortho and para isomers for diprotonation and dimethylation, respectively. Proton affinities and methyl cation affinities have been found to be additive in nature and these values also justify calculated thermochemical parameters. A correlation is observed between proton and methyl cation affinity with the change in enthalpy. Positive values of proton and methyl cation affinities proportionate to $-\Delta H$ values of the conversions and vice versa.

3.5 References and notes

1. Wheland, G. W. *J. Am. Chem. Soc.* **1942**, *64*, 900.
2. Olah, G. A.; Khun, S. J. *J. Am. Chem. Soc.* **1958**, *80*, 6535.
3. Olah, S.; Porter, M.; Kelley, M. *J. Am. Chem. Soc.* **1972**, *94*, 2034.
4. Gold, V.; Tye, F. L. *J. Chem. Soc.* **1952**, 2172.

5. Reid, C. *J. Am. Chem. Soc.* **1954**, *76*, 3264.
6. (a) Crestoni, M. E.; Fornarini, S. *J. Am. Chem. Soc.* **1994**, *116*, 5873. (b) Glukhovtsev, M. N.; Bach, R. D.; Bach, S.; Laiter, S. *J. Org. Chem.* **1997**, *62*, 4036. (c) Stock, L. M. *Aromatic Substitution Reaction*, Prentice-Hall, Englewood Cliffs, NJ, **1968**. (d) Terrier, F. *Nucleophilic Aromatic Displacement – The influence of the Nitro-group*, Feuer H. (Ed.), VCH publishers, New York, **1991**. (f) Chuparkhin, O. N.; Charushin, V. N.; Van Der Plas, H. C. *Nucleophilic Aromatic Substitution of H*, Academic Press, San Diego, **1994**. (g) Kryazev, V. N., Drozd, V. N. *Russ. J. Org. Chem.* **1995**, *31*, 1.
7. Hehre, W. J.; Pople, J. A. *J. Am. Chem. Soc.* **1972**, *94*, 6901.
8. Sumathy, R.; Kryachko, E. S. *J. Phys. Chem. A* **2002**, *106*, 510.
9. Roithova, J.; Schroder, D.; Berger, R.; Schwarz, H. *J. Phys. Chem. A* **2006**, *110*, 1650.
10. Raos, G.; Astorri, L.; Raimondi, M.; Cooper, D. L.; Gerrattand, J.; Karadakov, P. B. *J. Phys. Chem. A* **1997**, *101*, 2886.
11. Miklis, P. C.; Ditchfield, R.; Spencer, T. A. *J. Am. Chem. Soc.* **1998**, *120*, 10482.
12. Ishikawa, Y.; Yilmaz, H.; Yanai, T.; Nakajima, T.; Hirao, K. *Chem. Phys. Lett.* **2004**, *396*, 16.
13. Zheng, F.; Sa, R.; Cheng, Jiang, H.; Shen, J. *Chem. Phys. Lett.* **2007**, *435*, 24.
14. Polo, V.; Gräfenstein, J.; Kraka, E.; Cremer, D. *Theor. Chem. Acc.* **2003**, *109*, 22.
15. Johnson, B. G.; Gonzales, C. A.; Gill, P. M. W.; Pople, J. A.; *Chem. Phys. Lett.* **1994**, *221*, 100.
16. Eriksson, L. A.; Kryachko, E. S.; Nguyen, M. T.; *Int. J. Quantum Chem.* **2004**, *99*, 841.
17. Yang, W.; Morteir, W. J.; *J. Am. Chem. Soc.* **1986**, *108*, 5708.
18. Vos, A. M.; Schoonheydt, R. A.; De Proft, F.; Geerlings, P. *J. Catal.* **2003**, *220*, 333.
19. Chattaraj, P. K.; Maiti, B.; Sarkar, U. *J. Phys. Chem. A* **2003**, *107*, 4973.
20. Fukui, K.; Yonezawa, T.; Shingu, H. *J. Chem. Phys.* **1952**, *20*, 722.
21. Parr, R. G.; Yang, W. *J. Am. Chem. Soc.* **1984**, *106*, 404.
22. Yang, W.; Parr, R. G.; *Proc. Natl. Acad.* Sci. USA 826723. 1985.

23. Maksic, Z. B.; Maksic, M. E.; Knezevic, A. *J. Phys. Chem. A* **1998**, *102*, 2981.

24. Otto, A. H. *Phys. Chem. Commun.* **1999**, 12.

25. M.J. Frisch et al., GAUSSIAN 03 (Revision D.01) Gaussian, Inc., Wallingford, CT, **2004**.